Collective bubble oscillations as a component of surf infrasound

Joseph Park,[a] Milton Garcés, and David Fee
University of Hawaii, Infrasound Laboratory, 73-4460 Queen Kaahumanu Hwy #119, Kailua-Kona, Hawaii 96740, USA

Geno Pawlak
University of Hawaii at Manoa, Department of Ocean and Resources Engineering, 2540 Dole Street, Holmes Hall 404, Honolulu, Hawaii 96822, USA

(Received 14 June 2007; revised 13 November 2007; accepted 31 January 2008)

Plunging surf is a known generator of infrasound, though the mechanisms have not been clearly identified. A model based on collective bubble oscillations created by demise of the initially entrained air pocket is examined. Computed spectra are compared to infrasound data from the island of Kauai during periods of medium, large, and extreme surf. Model results suggest that bubble oscillations generated by plunging waves are plausible generators of infrasound, and that dynamic bubble plume evolution on a temporal scale comparable to the breaking wave period may contribute to the broad spectral lobe of dominant infrasonic energy observed in measured data. Application of an inverse model has potential to characterize breaking wave size distributions, energy, and temporal changes in seafloor morphology based on remotely sensed infrasound.
 [DOI: 10.1121/1.2885743]

PACS number(s): 43.28.Dm, 43.30.Bp, 43.30.Pc [WMC] Pages: 2506–2512

I. INTRODUCTION

Oceanic ambient noise arises from a diverse set of geophysical, biological, and mechanical sources. This paper focuses on characterization of infrasound (1–20 Hz) produced from ocean waves breaking on coastlines-surf. Wave breaking processes are important contributors to the acoustic ambient field. Above roughly 500 Hz breathing-mode oscillation of individual air bubbles entrained by breaking waves constitute an important underwater sound source,[1] while at frequencies below 500 Hz it has been shown that collective bubble oscillations are significant generators of acoustic power.[2–6] In the infrasonic band known contributors include turbulence, machinery, and wave-wave interactions.[7,8] Analysis of oceanic infrasound by Nichols (1986) led to speculation that breaking waves could be capable sources,[9] followed by McCreery and Duennebier (1993) who postulated that hydroacoustic energy in the 0.5–10 Hz band might be attributed to coastal wave breaking.[10] It has been shown that near surface infrasonic sources can couple with insignificant power loss into the atmosphere,[11] and several studies have verified surf as a persistent and significant source of atmospheric infrasound.[12–15]

The type of breaking wave exerts a large influence on the generation of low frequency sound. Wave tank observations by Loewen and Melville revealed that plunging waves generate low frequency ($f>20$ Hz) energy correlated with breaking, while spilling waves do not.[5] Likewise, measurement of individual coastal breaking waves by Garcés *et al.* found that plunging waves were effective infrasonic sources ($f<20$ Hz), whereas spilling breakers were not.[16] Plunging waves are characterized by an overturning jet (or wall) of water which plunges forward of the wave and completely encloses a pocket of air (the tube, or barrel), while spilling breakers collapse into a bore of foam. Therefore, one can speculate that the unique water jet impact and enclosed vortex generation of plunging waves are candidate mechanisms for infrasound generation.

Even though specific generation mechanisms for surf infrasound have not been clearly identified, the foregoing observations suggest several likely sources: hydraulic impact of the plunging wave jet,[17] oscillations of the plunging wave jet-splash cycle,[18] impulse pressure "bounce back" from hydraulic impacts on elastic bodies (cliffs, reefs, seafloor),[19] multiple coherent vortex structure generation under the wave,[20] breathing-mode oscillation of the initially enclosed air volume,[5] and the collective oscillation of the collapsing bubble plume,[16,21]

Regarding the collective oscillation mechanism as a low frequency source, Carey speculated "If the spatial distribution of bubbles is related to the vorticity distribution, then the noise due to collective oscillations should have frequencies determined by the size of the vorticities".[22] The primary aim of this paper is to investigate the collective bubble oscillation mechanism as a potential generator of infrasound from plunging surf with sufficient energy and spatial scales. A model is developed in which bubble plume distributions are estimated from breaking wave spectra. Plume oscillations and temporal evolution lead to an estimate of acoustic radiation frequency as a function of breaking wave frequency, which is transformed into a relative acoustic amplitude spectrum. Model results are compared to field data and some inferences regarding bubble plume evolutions are presented.

[a]Author to whom correspondence should be addressed. Electronic mail: jpark@isla.hawaii.edu

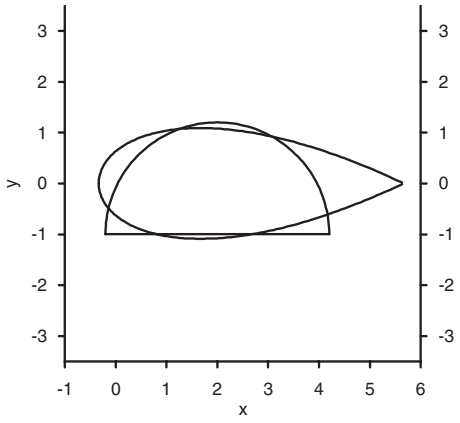

FIG. 1. Longuet-Higgins cubic vortex function compared to a semicylindrical cross section.

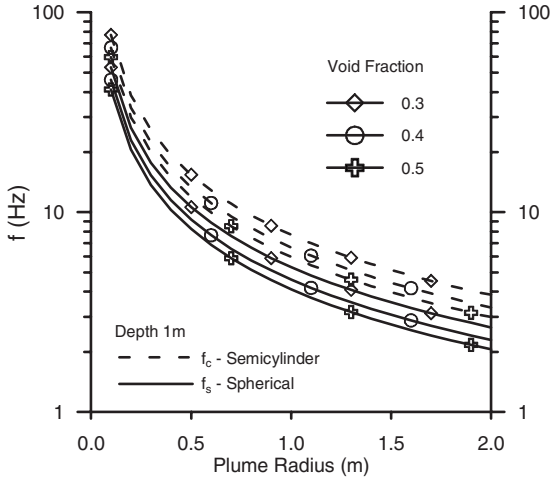

FIG. 2. Lowest eigenfrequency of collective bubble oscillation.

II. LOW FREQUENCY SOUND GENERATION FROM BUBBLE OSCILLATIONS

Wave breaking results in subsurface air entrainment which leads to both individual[5] as well as collective bubble oscillations,[2,4] each capable of generating low frequency acoustic radiation. According to Loewen and Melville, the low frequency sound produced by plunging waves contains two components.[5] The first is detected at the time of breaking and is attributed to "volumetric pulsation of the cylinder of pure air (100% void fraction) entrapped by the plunging wave crest." The second, which initiates some fraction of a wave period, later occurs when "the cylinder of pure air breaks up to form a bubble plume." It was noted by Loewen and Melville that the second component is a "slightly lower frequency signal" than the first.

Field observation and experiments indicate that the cross section of initial air entrainment by plunging waves is typically asymmetric.[5,23,24] Longuet-Higgins expressed the cross-section of the initial air volume in terms of a parametric cubic function with a shape resembling a teardrop (see Fig. 1).[23] Experimental work by Loewen and Melville found it convenient to model the bubble plume as a semicylindrical horizontal tube parallel to the crest of the wave.[5] As a comparison, Fig. 1 plots the Longuet-Higgins vortex function along with a semicylindrical cross section that has a radius the same dimension as the maximum vortex height.

Based on wave tank experiments Loewen and Melville fitted an empirical expression for the lowest eigenfrequency (see Fig. 2) of the semicylindrical horizontal bubble plume[5]

$$f_c \approx \frac{1}{2.5R_B}\sqrt{\frac{P_o}{\beta\rho}}, \tag{1}$$

where the range of approximation encompassed a plume radius R_B less than 1 m, and air volume fraction β less than 0.1. P_o denotes the ambient pressure and ρ the density of water. This expression is similar to that of the lowest eigenfrequency of a spherical cloud of radius R reported by Carey in Ref. 4

$$f_s = \frac{1}{2\pi R}\sqrt{\frac{3\gamma P_o}{\beta\rho}}, \tag{2}$$

where γ is the adiabatic ratio of specific heat. Comparison of Eqs. (1) and (2) reveals that $f_c \approx 1.45 f_s$, indicating that the asymmetric plume has a higher fundamental resonance than the spherical plume.

Using β values in the range measured by Deane,[24] $\gamma = 1$ (isothermal conditions, bubble surface tension is neglected), $P_o = 111{,}145$ Pa (depth 1 m) and $\rho = 1000$ kg/m^3, results of Eqs. (1) and (2) are shown in Fig. 2. These results indicate that for plunging breakers which produce approximately semicylindrical bubble clouds with characteristic radii larger than about 1/2 m, infrasonic generation from collective bubble oscillation is plausible.

III. ACOUSTIC MODEL

The model relies on a breaking wave spectrum to estimate the distribution of bubble plume sizes, which is transformed into an acoustic radiation spectrum. Considering only the entrained air oscillations, the model can be represented with a series of functional transformations applied to the deepwater wave spectrum.

Model input consists of a deepwater ocean wave spectrum $S(\omega)$ (Fig. 3), which can be constructed from wave

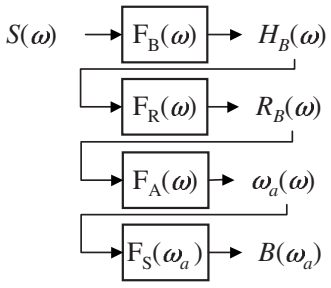

FIG. 3. Schematic of the acoustic transformation model: ω is the deepwater ocean wave frequency, ω_a the acoustic radiation frequency, S the deepwater wave spectrum, H_B the breaking wave height spectrum, R_B the bubble cloud characteristic length distribution and B the amplitude spectrum of acoustic radiation.

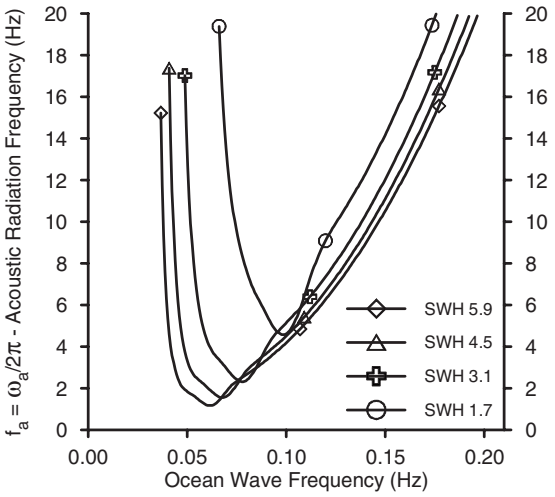

FIG. 4. Radiation frequencies of collective bubble oscillation from Eq. (6) versus the deepwater wave frequency for spectra with SWH of 1.7, 3.1, 4.5 and 5.9 m.

growth models applied to atmospheric weather conditions, or applied directly from observed ocean data buoys. The nonlinear transformation $F_B(\omega)$ produces a breaking wave height spectrum $H_B(\omega)$, which will depend on local bathymetry. $F_B(\omega)$ can be obtained from a breaker height index derived from empirical data,[25] or from a hydrodynamic wave model.[26] The breaking wave spectrum is then converted to a spectrum of bubble cloud characteristic lengths, $R_B(\omega)$, by the function $F_R(\omega)$ which can be modeled from data relating bubble cloud distributions to breaking wave height[27] and temporal evolution of plume dynamics.[6] The bubble cloud dimension is transformed into spectrum of acoustic radiation frequencies, $\omega_a(\omega)$ (see Fig. 4), based on the nonlinear transformation $F_A(\omega)$ which accounts for the radiation characteristics of the bubble plume.[5] Note that the deepwater wave frequency is denoted by ω, while the acoustic radiation frequency is denoted ω_a. Finally, the nonlinear distribution of radiation frequencies is summed and scaled across the acoustic frequency spectrum to estimate the acoustic radiation spectrum $B(\omega_a)$. Figure 3 is a schematic diagram of the model.

A. Breaking wave height spectrum

In the current model we employ the JONSWAP spectrum[28] as the deepwater wave generator, although other suitable distributions can be used. Median values of JONSWAP spectrum parameters were used (peak enhancement factor $\gamma=3.3$, peak width factor $\sigma=0.08$.) Model input consists of wind speed and fetch, from which the deepwater wave spectrum $S(\omega)$ is computed.

The function $F_B(\omega)$ transforms the deepwater wave spectrum into a breaking wave spectrum: $H_B(\omega)=F_B(S(\omega))$. One way to quantify the transition from deepwater-to-breaking wave height is with the breaker height index $h_B=H_B/H_o$ where H_B is the breaking wave height and H_o the deepwater wave height.[25] The breaker height index depends on beach slope and the incident wave steepness H_o/L_o, where L_o is the wavelength, and can be described with a power law of the form

$$h_B = c(H_o/L_o)^{-d} \tag{3}$$

with parameters $c=0.5784$, $d=0.23925$ for a beach slope of 1/10, and $c=0.5403$, $d=0.21618$ for a beach slope of 1/50.

Given a deepwater wave spectrum and slope of the beach where breaking will occur, a breaker height spectrum can be estimated by multiplying the deepwater spectrum with the corresponding breaker height index at each frequency.

$$H_B(\omega) = h_B(\omega) \cdot S(\omega) \tag{4}$$

With an estimate of the breaking wave spectrum at hand, the next step is to relate the breaking wave distribution to bubble cloud dimensions.

B. Bubble plume distribution

Application of Eq. (1) to estimate the acoustic spectrum of collective bubble radiation requires specification of the bubble plume radius, R_B, for each wave of the spectrum. Based on similarity between the Longuet-Higgins vortex function and a semicylinder of comparable scale (Fig. 1), the model assumes that the vortex height H_v, can be used as an approximation to the semicylindrical radius of Eq. (1). We therefore seek a variable, C_H, which scales the breaking wave height into an equivalent vortex height as shown in Eq. (5).

$$R_B(\omega) = H_v(\omega) = C_H \cdot H_B(\omega). \tag{5}$$

Mead and Black quantified ratios of vortex to breaking height at 26 surf locations,[27] from which we compute a mean value of $C_H=0.37$. The model estimate of initially entrained vortex height is therefore specified as: $H_v(\omega)=0.37 \cdot H_B(\omega)$.

C. Bubble radiation

The model assumes that the fundamental frequency f_c specified in Eq. (1) scales to plume dimensions larger than $R_B \approx 1$ m. This assumption is based on the scale invariance observed between Eqs. (1) and (2) in Fig. 2 as R exceeds 1 m. A spectrum of acoustic radiation frequencies associated with each incident breaking wave frequency can then be computed by combination of Eqs. (1) and (5):

$$\omega_a(\omega) = \frac{2\pi}{2.5H_v(\omega)}\sqrt{\frac{P_o}{\beta\rho}}. \tag{6}$$

Equation (6) does not quantify the spectral amplitude of radiation, rather, it defines a mapping between an incident breaking wave frequency and an estimate of the frequency of radiation of the collapsing vortex. Estimates of relative spectral amplitude are addressed in the next section.

To examine the evolution of bubble radiation with changes in wave group energy, Fig. 4 plots radiation frequencies of Eq. (6) for ocean wave spectra with deepwater significant wave heights of 1.7, 3.1, 4.5 and 5.9 m. As ocean wave group energy increases, with a corresponding increase in dominant wavelength and height, the acoustic radiation

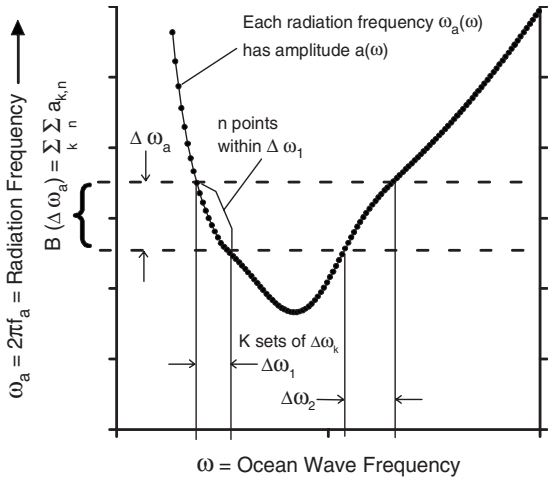

FIG. 5. Schematic of multiple contributions to bubble spectrum ω_a from ocean waves of different frequencies ω.

frequencies deepen into lower values. Thus we expect acoustic radiation spectra to exhibit stronger low frequency energy as incident ocean wave energy increases. One can also observe that the acoustic radiation broadens, covering a wider range of incident wave frequencies. This suggests that as incident wave energy increases, the acoustic radiation spectrum should also broaden around its main energy lobe.

D. Spectral amplitude estimates

The acoustic radiation frequencies of the model are computed from Eq. (6), we seek to transform this spectrum of radiation frequencies (such as shown in Fig. 4 where $\omega_a = 2\pi f_a$) into a spectrum of acoustic radiation amplitude, $B(\omega_a)$. The task is to identify the amplitude coefficient, B, associated with each acoustic radiation frequency ω_a.

It is clear from the nonlinear nature of $\omega_a(\omega)$ in Fig. 4 that bubble oscillations induced from multiple ocean wave frequencies can contribute to a single value of ω_a, and therefore B. This reflects the fact that for a given wave spectra, there can exist two frequencies with the same wave height. To account for these multiple sources, denote the acoustic radiation amplitude coefficient from each of k contributing ocean wave frequency as $a_k(\omega)$. In relation to Fig. 4 there are two contributing ocean waves at most values of ω_a, so that values of k are 1 and 2.

From an engineering perspective, there are a finite number of points in the spectra ω_a and B, and we denote the analysis binwidth of each component of B as $\Delta\omega_a$. Within each $\Delta\omega_a$ we designate the number of points for each of the k components as n. With an assumption of superposition, the discrete value of B within each analysis binwidth is given by

$$B(\Delta\omega_a) = \sum_k \sum_n a_{k,n}. \tag{7}$$

Figure 5 depicts the application of Eq. (7) to a representative radiation frequency spectrum $\omega_a(\omega)$.

Failure of superposition would arise from destructive interference between multiple, independent sources radiating at ω_a. However, the ocean wave periods and temporal persistence of the bubble plumes are an order of magnitude greater than the periods of ω_a. Given detector integration windows which are significantly greater than the wave period, it can be assumed that phase components are uniformly distributed and the amplitudes will be additive.

It is likely that a is a multiparametric function not just dependent on ω, but also a function of wave energy, site-specific wave breaking parameters such as beach slope, and other factors. Ideally, an estimate of the amplitude could be made from a low frequency acoustic model which considers both the bubble oscillation mechanics and the source-receiver transfer functions. For example, in the ocean layer the low frequency bubble oscillation models of Oguz[29] or Means[30] might assess the integrated behavior of the bubble plumes, while an additional aeroacoustic transfer function would be needed to model the atmospheric propagation to the infrasonic sensors. However, application of such models is beyond the scope of the present effort, and, it is useful to assess to what extent a simple first-order model can provide a robust and efficient estimator of breaking wave energy from remotely monitored infrasound. Here we make the assumption that $a(\omega)$ decays according to a simple $1/f$ scaling

$$a_n = A_n / f_{a_n}, \tag{8}$$

where A is a coefficient which can be used to describe the amplitude factors derived from higher order models such as those by Oguz[29] and Means,[30] and which can account for corrections due to the density of points summed in $\Delta\omega_a$. The discrete magnitude coefficients of B are then specified by

$$B(\Delta\omega_a) = \sum_k \sum_n A_{k,n} / f_{a_{k,n}}. \tag{9}$$

In the current model, $A \equiv 1$, and consequently this model is incapable of predicting absolute spectrum levels, it is limited to characterization of cutoff frequencies and spectral shape.

E. Bubble plume evolution

Bubble plumes from breaking ocean waves are known to persist for time scales on the order of seconds to tens of seconds. Given the dynamic environment in which the plumes are formed, and the unbalanced nature of the forces, plumes can evolve significantly within relatively short time scales (fractions of wave period). Two of the primary changes are a decrease in plume entrained air fraction, β, and an increase in plume cross-sectional area. Other important features include the horizontal and vertical velocities of the plume.

Lamarre and Melville[6] quantified plume dynamics in wavetank measurements and reported statistical moments of plume evolution. The mean void fraction as a function of time exhibited a nearly linear decrease for approximately one-half wave period after breaking. Based on their results, we have applied the following relationship to model the void fraction evolution:

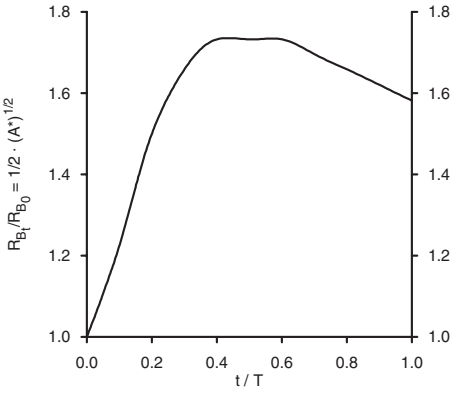

FIG. 6. Approximate evolution of plume cross-sectional area.

$$\beta(t) = \beta(0) - \frac{0.56t}{T};\ t \leqslant \frac{T}{2}, \tag{10}$$

where T is the wave period and $\beta(0)$ the initial air void fraction.

The bubble plume cross-sectional area normalized by the initial volume per unit width $(A*)$ was also reported as a function of time. It exhibited a nearly linear increase for the first several tenths of wave period after breaking, then tended to flatten out, and eventually decrease after times comparable to a wave period. There was considerable scatter in the data for times greater than about 0.2 T.

Equation (5) defines the initial bubble plume radius $R_B(\omega,t=0)$ as a function of breaking wave height. To model the evolution of plume radius, R_B is modulated with the relative radius length scale $\sqrt{A*}/2$

$$R_B(\omega,t) = \frac{\sqrt{A*(t)}}{2} R_B(\omega,t=0). \tag{11}$$

Values of $R_B(\omega,t)$ are then applied in Eq. (6) as the vortex height H_v to model time-varying plume growth. Figure 6 plots the evolution of the relative plume radius $\sqrt{A*}/2$, where values of $A*$ were taken from Ref. 6.

IV. KAUAI DATA

Figure 7 plots atmospheric infrasound recorded at a nearshore inland location on the island of Kauai during periods of moderate, high and extreme surf over the period March 4–March 10, 2005.[12] The spectra are parameterized in terms of significant wave height (SWH) measured from seafloor mounted pressure sensors offshore the surf zone. As the SWH increases there is a general increase in sound level, a shift to lower frequencies of the dominant energy, and a broadening of the dominant energy lobe. These observations are consistent with expectations of spectral evolution suggested by the computed radiation frequency spectra of Fig. 4.

Signal processing of the raw infrasound data collected at Kauai used an integration window of $\tau=3600$ s to estimate the spectral levels presented in Fig. 7. Since the model is based on transformation of radiation frequencies derived from a complete breaking wave distribution, model predictions are relevant only if the data window has sufficient length to sample a significant proportion of wavenumbers

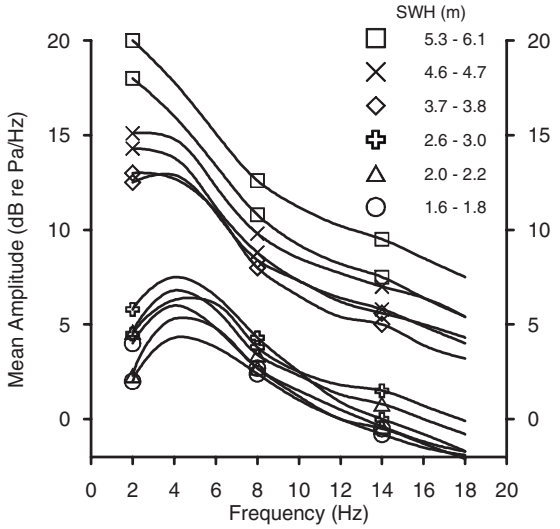

FIG. 7. Atmospheric infrasound from waves breaking at Polihale, Kauai.

represented in the breaking wave distribution. Most of the energy in the ocean wave spectra are contained in the 0.05–0.1 Hz bands, with dominant frequencies in the range 0.06–0.09 Hz corresponding to periods of 11–17 s. The long integration windows of the Kauai data allow for over 150 events with a period of 20 s, and therefore are deemed appropriate for model comparison.

V. MODEL RESULTS

This section presents comparisons of model results with measured data. Parameters used in model runs are as follows:

1. Slope of the breaking wave seafloor $m=0.06$.
2. Initial plume void fraction $\beta_0=0.35$, consistent with measured values by Deane.[24]
3. Initial vortex breaking height ratio $C_H=0.37$, from Sec. III B, Eq. (5).
4. Radiation spectrum (f_a) amplitude analysis binwidth $\Delta\omega_a=0.5$ Hz.

In default mode the model assumes that bubble plumes are static, there is a single bubble distribution that is summed in Eq. (9) to estimate the spectral shape. The model is capable of including contributions from additional bubble distributions according the evolution Eqs. (10) and (11). With this dynamic plume option, the void fraction values are decreased according to Eq. (10), and the plume effective radius is increased according to Eq. (11). Contributions for additional plumes in Eq. (9) are evaluated at fractional wave periods $t/T=0.1,0.2,0.3,0.4,0.5$.

Figure 8 plots results of Eq. (9) corresponding to deep-water significant wave heights of 1.8, 2.1, 2.4, 2.8, 3.7 and 4.6 m. Since the model computes only relative spectral levels, a bias term has been added to each computed spectrum to match the 10 Hz value of observed data.

Concerning the medium to large scale surf (SWH 1.8–2.4 m) represented in Fig. 8, characterization of the dominant infrasonic frequency is reasonable. This indicates that the presumed bubble oscillation mechanism is a candi-

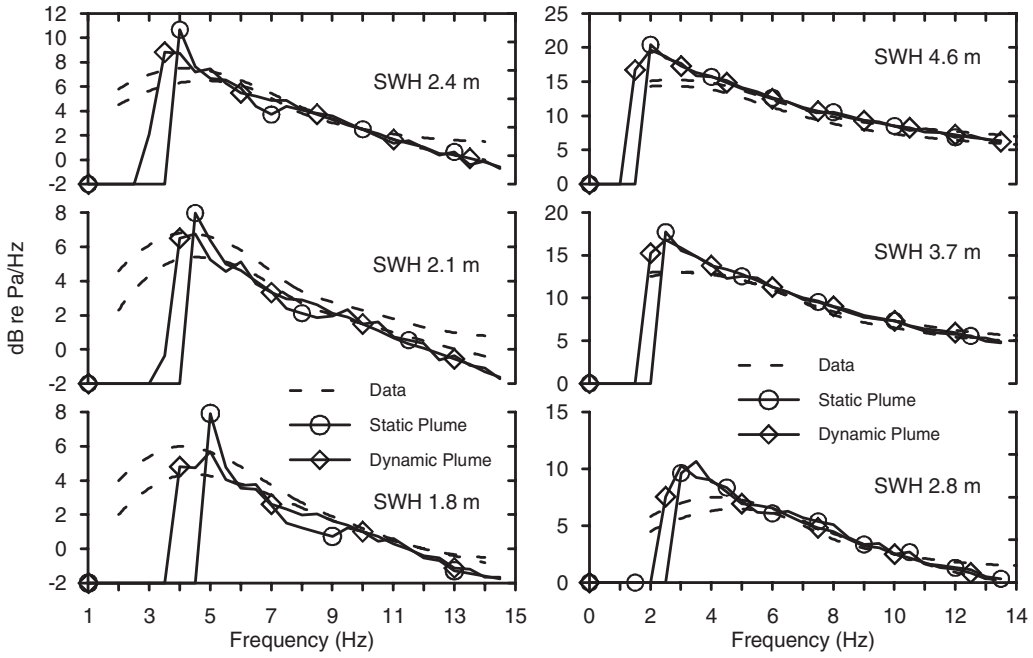

FIG. 8. Modeled infrasound spectra for ocean wave spectra with SWH of 1.8, 2.1, 2.4, 2.8, 3.7, 4.6 m compared to Kauai data.

date mechanism for generation of surf infrasound. It is also observed that the dynamic plume approximation has a broader main lobe, and lower cutoff frequency than the static plume, which is consistent with a larger sample of plume distributions that grow in size as the plume evolves. This result suggests that dynamic plume evolution is a significant factor contributing to the broad spectral lobes of dominant energy observed in field data.

Model results for the large and extreme surf conditions (SWH $>$ 2.5 m) estimate spectral shapes similar to the data, again with a slightly broader, lower frequency main energy lobe with the dynamic plume approximation. Prominence of the main energy lobe diverging from the spectral shape of the observed data may indicate that at these large spatial scales and energies the collective bubble oscillation mechanism is not a dominant contributor to infrasound generation. In this regime, the impact mechanisms may play a larger role.

VI. DISCUSSION

It has been recognized that remotely sensed infrasound has potential to provide "useful insight into coastal processes and permit an assessment of wave energy distribution in the littoral zone".[31] Indeed, Aucan *et al.* demonstrated that the bandpassed time series envelope of atmospheric infrasound generated by plunging surf can be used to estimate the dominant breaking wave period.[32] As an extension, we propose that based on an infrasound model such as that described above, an inverse model could be used to estimate a breaking wave height spectrum $H_B(\omega)$ from a measured infrasound spectrum $B(\omega_a)$.

Not only can an estimate of $H_B(\omega)$ be obtained, but one should also be able to estimate the bubble plume size distribution $R_B(\omega)$. Lamarre and Melville[33] found that dissipation of breaking ocean wave energy by air entrainment against buoyancy can account for up to 50% of the dissipated energy. Therefore, with an estimate of the initial wave energy spectrum and the entrained air volumes, the wave energy dissipated in breaking might be estimated. The residual could provide an estimate of the wave energy available for runup on the shore.

Another potential assessment of littoral dynamics is long term monitoring of surf zone bathymetric changes. Since bathymetry is a key variable in determination of the breaking wave spectrum, it is conceivable that parametric model fits to long term infrasonic monitoring could characterize seafloor morphology over times cales of days to months.

VII. CONCLUSION

A simple, functional transformation model of infrasound generated by collective bubble oscillations from collapsing air pockets entrained by plunging surf has been developed. The model is limited to estimation of relative spectral shape and cutoff frequencies since the amplitude coefficients of radiating spectral components are not quantified. Application of low frequency models which characterize the amplitude distributions, and source-receiver transfer functions[29,30] have potential to remove this limitation. Nonetheless, the model captures the observed characteristics of surf infrasound which include migration of dominant infrasonic energy to lower frequencies as ocean wave energy increases, and a broadening of the infrasonic energy distribution across the main lobe.

The model matches dominant infrasound frequencies and spectral shape reasonably well for medium to large scale surf, which may indicate that collective bubble oscillations are effective generators of surf infrasound. Further, it is suggested that dynamic plume evolution between breaking events is crucial to produce the observed broad spectral lobe around the dominant frequency of infrasonic energy. At the large and extreme scales of wave breaking, for example

when breaking wave heights exceed roughly 5 m, the model overestimates the relative amplitude of the lowest frequency components of the infrasound. This may indicate that at these larger spatial scales and energies the collective bubble oscillation mechanism is less important. In this regime hydrodynamic sources such as jet impact, vortex generation, impulse pressure bounce back, impact reverberations, as well as the massive bores of foam which persist shoreward of the plunging surf zone are potential contributors.

Estimation of acoustic radiation spectra from deepwater ocean wave spectra (forward model) constitutes a nonlinear transformation. Inversion of this model, for example with a neural network or other nonlinear state estimator, has potential to characterize surf-zone hydraulic and geomorphic dynamics based on remote infrasound sensing. In particular, it is suggested that the breaking wave height distribution, wave energy dissipation, wave energy runup potential, and long term bathymetric dynamics could be assessed.

ACKNOWLEDGMENT

The authors thank Dr. Robert M. Kennedy for his thoughtful review of the manuscript and suggestions which served to improve the paper.

[1]W. K. Melville, "The role of surface-wave breaking in air-sea interaction," Annu. Rev. Fluid Mech. **28**, 279–321 (1996).
[2]A. Prosperetti, "Bubble-related ambient noise in the ocean," J. Acoust. Soc. Am. **78**(S1), S2 (1985).
[3]A. Prosperetti, "Bubble-related ambient noise in the ocean," J. Acoust. Soc. Am. **84**(3), 1042–1054 (1988).
[4]W. Carey, "Low frequency noise from breaking waves," *Natural Physical Sources of Underwater Sound: Sea Surface Sound (2)*, edited by B. R. Kerman. (Kluwer Academic, Dordrecht, 1993).
[5]M. R. Loewen and W. K. Melville, "An experimental investigation of the collective oscillations of bubble plumes entrained by breaking waves," J. Acoust. Soc. Am. **95**(3), 1329–1343 (1994).
[6]E. Lamarre and W. K. Melville, "Void fraction measurements and sound-speed fields in bubble plumes generated by breaking waves," J. Acoust. Soc. Am. **95**(3), 1317–1328 (1994).
[7]S. C. Webb, "Broadband seismology and noise under the ocean," Rev. Geophys. **36**(1), 105–142 (1998).
[8]A. C. Kibblewhite and K. C. Evans, "Wave-wave interactions, microseisms, and infrasonic ambient noise in the ocean," J. Acoust. Soc. Am. **78**(3), 981–994 (1985).
[9]R. H. Nichols, "Infrasonic ocean noise sources: Wind versus waves," J. Acoust. Soc. Am. **82**(4), 1395–1402 (1987).
[10]C. S. McCreery and F. K. Duennebier, "Correlation of deep ocean noise (0.4–30 Hz) with wind, and the Holu Spectrum—A worldwide constant," J. Acoust. Soc. Am. **93**(5), 2639–2648 (1993).
[11]O. A. Godin, "Anomalous transparency of water-air interface for low-frequency sound," Phys. Rev. Lett. **97**, 164301 (2006).
[12]M. Garcés *et al.*, "Infrasound from large surf," Geophys. Res. Lett. **33**, L05611 (2006).
[13]S. J. Arrowsmith and M. A. H. Hedlin, "Observations of infrasound from surf in southern California," Geophys. Res. Lett. **32**, L09810 (2005).
[14]A. Le Pichon, V. Maurer, D. Raymond, and O. Hyvernaud, "Infrasound from ocean swells observed in Tahiti," Geophys. Res. Lett. **31**, L19304 (2004).
[15]M. Garcés, C. Hetzer, M. Merrifield, M. Willis, and J. Aucan, "Observations of surf infrasound in Hawaii," Geophys. Res. Lett. **30**, 2264 (2003).
[16]M. Garcés, D. Fee, S. McNamara, J. Aucan, and M. Merifield, "The deep sound of one wave plunging," J. Acoust. Soc. Am. **120**(5), 3032 (2006).
[17]D. H. Peregrine, "Breaking waves on beaches," Annu. Rev. Fluid Mech. **15**, 149–178 (1983).
[18]J. A. Battjes, "Surf-zone dynamics," Annu. Rev. Fluid Mech. **20**, 257–291 (1988).
[19]D. H. Peregrine, "Water-wave impact on walls," Annu. Rev. Fluid Mech. **35**, 23–43 (2003).
[20]Y. Watanabe, H. Saeki, and R. J. Hosking, "Three dimensional vortex structures under breaking waves," J. Fluid Mech. **545**, 291–328 (2005).
[21]D. Fee *et al.*, "Advances in surf infrasound monitoring," *2006 Infrasound Technology Workshop, Geophysical Institute, University of Alaska, Fairbanks*, September 25–28 (2006).
[22]W. Carey, "Low-to mid-frequency oceanic noise," *Natural Physical Processes Associated with Sea Surface Sound*, edited by T. G. Leighton, (University of Southampton, Southampton, 1997).
[23]M. S. Longuet-Higgins, "Parametric solutions for breaking waves," J. Fluid Mech. **121**, 403–424 (1982).
[24]G. B. Deane, "Sound generation and air entrainment by breaking waves in the surf zone," J. Acoust. Soc. Am. **102**(5), 2671–2689 (1997).
[25]U. S. Army Coastal Engineering Research Center, *Shore Protection Manual, Volume 1* (U. S. Government Printing Office, Washington D.C., 1977).
[26]N. Booij, R. C. Ris, and L. H. Holthuijsen, "A third-generation wave model for coastal regions, Part I, Model description and validation," J. Geophys. Res., [Oceans] **104**, 7649–7666 (1999).
[27]S. Mead and K. Black, "Predicting the breaker intensity of surfing waves," J. Coastal Res. Special Issue No. 29, 51–56 (2001).
[28]K. Hasselmann, W. Sell, D. B. Ross, and P. Müller, "A parametric wave prediction model," J. Phys. Oceanogr. **6**, 200–228 (1976).
[29]H. N. Oguz, "A theoretical study of low-frequency oceanic ambient noise," J. Acoust. Soc. Am. **95**(4), 1895–1912 (1994).
[30]S. L. Means, "Low-frequency sound generation from breaking surf," Acta Radiol. **5**(2), 13–18 (2004).
[31]M. Garcés, D. Fee, P. Caron, C. Hetzer, J. Aucan, M. Merrifield, R. Gibson, and J. Bhattacharyya, "Multiparameter studies of surf infrasound," J. Acoust. Soc. Am. **117**(4), 2452 (2005).
[32]J. Aucan, D. Fee, and M. Garcés, "Infrasonic estimation of surf period," Geophys. Res. Lett. **33**, L05612 (2006).
[33]E. Lamarre and W. K. Melville, "Air entrainment and dissipation in breaking waves," Nature (London) **351**, 469–472 (1991).